

Hot carrier recombination model of visible electroluminescence from metal–oxide–silicon tunneling diodes

C. W. Liu,^{a)} S. T. Chang, W. T. Liu, Miin-Jang Chen,^{b)} and Ching-Fuh Lin^{b)}
Department of Electrical Engineering, National Taiwan University, Taipei, Taiwan

(Received 26 June 2000; accepted for publication 16 October 2000)

We report the visible electroluminescence at room temperature from metal–oxide–silicon tunneling diodes. As biased in the Fowler–Nordheim regime, the electrons tunnel from the gate electrode through the ultrathin oxide and reach the Si anode with sufficiently high energy. The hot electrons cause the impact ionization, and generate the secondary hot electrons and hot holes in Si substrates. The visible light comes from the radiative recombination between the secondary hot electrons and hot holes, and the hot carrier recombination model can fit the visible electroluminescence spectra.
 © 2000 American Institute of Physics. [S0003-6951(00)02751-0]

Continuous attempts have been made to realize viable light sources on Si, and the integration of light emitters and detectors in the metal–oxide–silicon (MOS) compatible process makes the optical interconnects feasible for ultralarge scale integration circuits.^{1,2} The study in the past was focused on the structure of *p–n* junctions. Two different Si light emitters have been reported using *p–n* diodes. A narrow-band infrared emitter at 1160 nm was implemented using a *p–n* junction under forward bias.³ A broadband (450–850 nm) visible-light emitter was also realized using an avalanche *p–n* diode.^{3,4} This visible light emission from the avalanche bias of *p–n* diodes has been explained by a Bremsstrahlung model,⁵ an intraconduction band recombination model,⁶ and a hot electron recombination model.⁷

Recently, MOS tunneling light emitting diodes have also shown the infrared band edge electroluminescence (EL)⁸ at accumulation bias. There are also reports on visible EL from MOS structures, and the origin has been attributed to oxide defects⁹ and hot electrons.¹⁰ In this letter, we report that a hot carrier recombination due to the impact ionization of the tunneling hot electron is responsible for the visible emission and the line shape of the visible emission can be fitted by this model.

The ultrathin gate oxide of the MOS tunneling diode used in this study is grown by rapid thermal oxidation (RTO) at 900 °C. The gas flows are 500 sccm nitrogen and 500 sccm oxygen at the pressure of 250 mbar. Before oxidation, the sample was cleaned by a HF dip. An *in situ* hydrogen bake at 900 °C for 2 min was performed before the growth of the RTO. The temperature was measured by a pyrometer with a close loop control. Although the interface state density of Si/oxide interface cannot be accurately measured by the capacitance–voltage method due to the gate leakage current, the measurement on dark current of the similar devices¹¹ and on thick oxide samples indicates that the interface state density is within $1 \times 10^{11} \text{ cm}^{-2}$. The nominal thickness of the oxide is about 3 nm, measured by ellipsometry. The resistivity of the 100 mm *p*-type (100) wafers is

1–10 Ω cm. The N (*n*-type) MOS diodes have an indium tin oxide (ITO) gate electrode with circular areas of $4 \times 10^{-2} \text{ cm}^2$ defined by photolithography. The visible light can pass the transparent ITO gate electrode and the detection signal can be increased. Note that for nontransparent electrode, a special structure is needed to observe the visible light from the edge of the MOS diodes with poly Si electrodes.¹⁰

For the ITO gate under negative bias, the electron in the ITO tunnels to the Si substrate through the thin oxide. The negative gate bias also attracts the hole at the Si/SiO₂ interface to form an accumulation region. At sufficiently large negative gate bias (>6 V), visible light is observed as shown in Fig. 1. Since visible EL has a very broad spectrum, corrections due to the sensitivity of photomultiplier tube (PMT) and the grating efficiency have to be taken into account. Figure 1 shows both the raw data obtained directly from the photomultiplier tube and the processed data after such corrections. The inset of Fig. 1 is the detector sensitivity and grating efficiency used for such corrections. The cutoff of the PMT is around 800 nm (1.55 eV). The raw data show a peak around 600 nm, but the processed data do not. This indicates the necessity of such corrections.

Figure 2 shows the visible spectra after corrections at different bias. The emission intensity increases with increasing bias voltage. The radiative recombination between tunneling electrons and accumulated holes seems unlikely re-

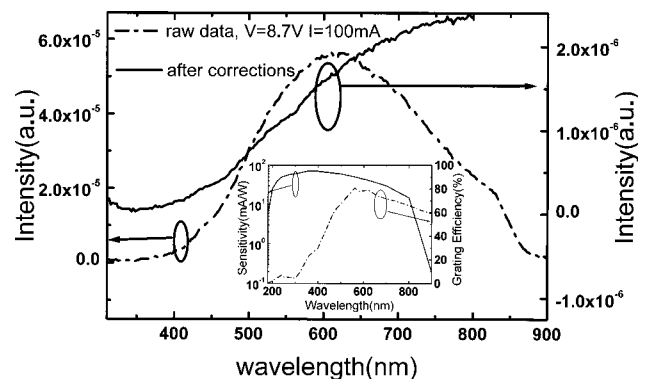


FIG. 1. The visible emission spectrum before and after corrections from MOS tunneling diodes. The inset is the detector sensitivity and grating efficiency used for corrections

^{a)}Also at Graduate Institute of Electronic Engineering; electronic mail: chee@cc.ee.ntu.edu.tw

^{b)}Also at: Institute of Electro-Optical Engineering.

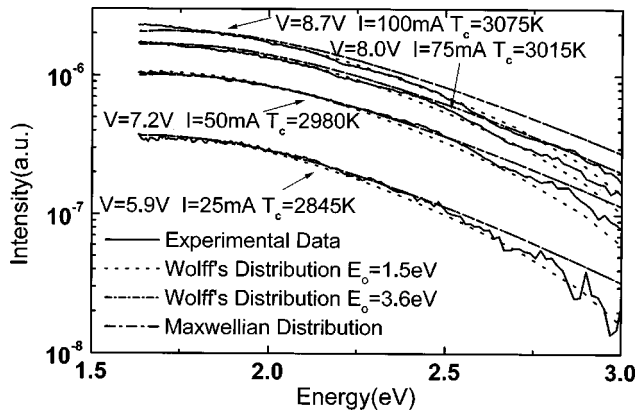


FIG. 2. The measured visible spectra from MOS tunneling diodes with ITO gates and the theoretical line shape from the hot carrier recombination model. Note that the theoretical curves using quasi-Maxwellian distribution are overlapped with those using Wolff's distribution with $E_0=3.6$ eV.

sponsible to the visible emission, since the spectra does not change significantly in shape as the negative gate bias increases from the 5.9 to 8.7 V.¹⁰ The energy of tunneling electrons reaching Si increases with the increasing gate voltage. The high-energy portion of the spectra would be more and more significant as the negative gate bias increases if the tunneling hot electrons recombined directly with holes. As reaching the Si, the tunneling electron has sufficient energy to cause the impact ionization at high negative gate voltage. The secondary hot electrons and holes are produced by the impact ionization (Fig. 3). The hot electron distribution function due to the impact ionization has been derived by Wolff¹² and is given by

$$f(E) \propto \exp(-\beta E) [1 - E_i(\beta E)/E_i(\beta E_0)],$$

where $E_i(x) = \int_{-\infty}^x [\exp(v)/v] dv$, $\beta = 1/k_B T_e$, T_e is the temperature, and E_0 is the ionization threshold to generate the secondary electrons and holes. The Wolff's distribution substantially below the ionization threshold is quasi-Maxwellian, and the electron temperature can be much higher than the lattice temperature.¹² Two different values of the impact ionization threshold of electrons were used in the

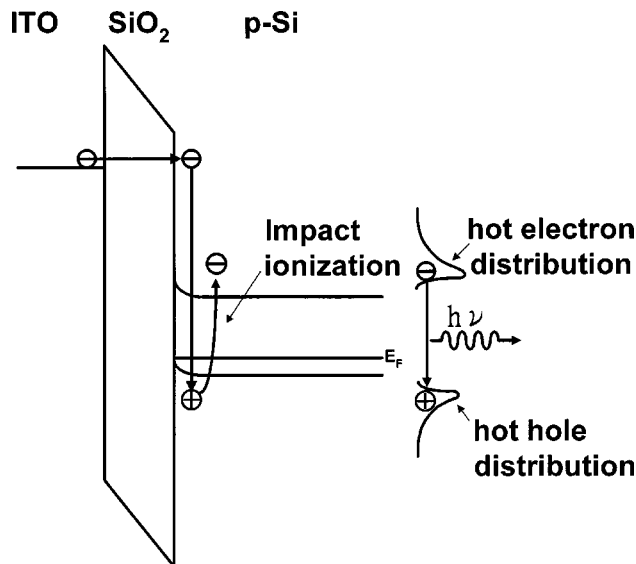


FIG. 3. The schematic diagram of the hot carrier recombination model.

literature. One is one and half of Si band gap,^{7,13} the other one is 3.6 eV.¹⁴ For the photon energy interested (1.5–3 eV), the Wolff's distribution is very close to quasi-Maxwellian if the 3.6 eV is used for ionization threshold. Due to the large density of states and large ionization threshold of holes (5.0 eV),¹⁴ the hot hole distribution function is commonly represented as quasi-Maxwellian.^{7,13} Similar to the electron-hole plasma recombination model,⁸ the momentum conservation in the indirect band gap Si is assumed to be conserved by impurity scattering, roughness scattering, and other mechanisms.⁸ The emission line shape is a simple convolution between electron and hole populations. Since the signal of the PMT detector is photon energy, not photon count, a photon energy weighting factor ($h\nu$) is also included in the hot carrier recombination model, which is

$$I(h\nu) = I_0 \int_0^{h\nu - E_g} h\nu D_e(E) D_h(h\nu - E_g - E) \\ \times f_e(E, T_e) f_h(h\nu - E_g - E, T_h) dE,$$

where D_e and D_h are the densities of states of electron and hole, respectively, $h\nu$ is the energy of photon emitted, E_g is the Si band gap, T_e and T_h are the hot electron and hot hole temperatures, respectively, the electron distribution function f_e is Wolff's, and hole distribution function f_h is quasi-Maxwellian. Figure 2 shows the theoretical curves of the emission line shape, which give the reasonable fit of experimental data. The theoretical line shape drops more slowly if the electron distribution function is quasi-Maxwellian as compared to the Wolff's distribution with $E_0=1.5$ eV. Note that the theoretical curves using quasi-Maxwellian electron distribution are overlapped with those using Wolff's distribution with $E_0=3.6$ eV in Fig. 2. For simplicity, we used the same T_e and T_h in the fitting. The carrier temperature increases from 2845 to 3075 K as the bias increases from 5.9 to 8.7 V. This indicates that the higher energy of tunneling electrons can produce secondary hot carriers with higher energy, and thus leads to higher carrier temperature. The ionization threshold of 1.5 eV gives a better fit than 3.6 eV in Fig. 2. For PMOS diodes (n -type substrate), no visible light was detected. This is probably due to the much lower impact ionization rate of holes¹⁴ in Si, as compared to electrons. The tunneling hole from the gate electrodes into Si substrates cannot produce sufficient hot electron and hot hole populations, and therefore, the visible light is too weak to be detected.

A visible light is observed from MOS tunneling diodes with ITO gates. The similar emission spectra have been observed in p - n junction under an avalanche bias. The origin of the emission in p - n junctions has been attributed to different mechanisms such as the Bremsstrahlung effect, the intraconduction recombination, and the hot carrier recombination and is still under debate. We, however, demonstrate that the visible emission in MOS structures is due to the hot carrier recombination, which are generated by high-energy electron tunneling from electrodes to p -type Si as biased in the Fowler-Nordheim regime. The theoretical line shape fits the experimental data reasonably well.

This work is supported by National Science Council, Taiwan, Republic of China (89-2218-E-002-017, 89-2218-E-

002-012, 89-2112-M-002-034, and 89-2215-E-002-016). The support from the Yen Tjing Ling Foundation is also highly appreciated.

- ¹K. Misiakos, E. Tsoi, E. Halmagean, and S. Kakabakos, *Tech. Dig. Int. Electron Devices Meet.* **25** (1998).
- ²C. W. Liu, M. H. Lee, C. F. Lin, I. C. Lin, W. T. Liu, and H. H. Lin, *Tech. Dig. Int. Electron Devices Meet.* **749** (1999).
- ³J. Kramer, P. Seitz, E. F. Steigmeier, H. Auderset, and B. Delley, *Sens. Actuators A* **37–38**, 527 (1993).
- ⁴L. W. Snyman, M. du Plessis, E. Seevinck, and H. Aharoni, *IEEE Electron Device Lett.* **20**, 614 (1999).
- ⁵T. Figielsky and A. Torun, *Proceedings of the International Conference on the Physics of Semiconductors, Exeter, UK, 1962*, p. 853.
- ⁶J. Bude, N. Nano, and A. Yoshii, *Phys. Rev. B* **45**, 5848 (1992).
- ⁷A. T. Obeidat, Z. Kalayjian, A. G. Andreou, and J. B. Khurgin, *Appl. Phys. Lett.* **70**, 470 (1997).
- ⁸C. W. Liu, M. H. Lee, M.-J. Chen, I. C. Lin, and C.-F. Lin, *Appl. Phys. Lett.* **76**, 1516 (2000).
- ⁹J. Yuan and D. Haneman, *J. Appl. Phys.* **86**, 2358 (1999).
- ¹⁰R. Versari, A. Pieracci, M. Manfredi, G. Soncini, P. Bellutti, and B. Ricco, *Tech. Dig. Int. Electron Devices Meet.* **745** (1999).
- ¹¹C. W. Liu, W. T. Liu, M. H. Lee, W. S. Kuo, and B. C. Hsu, *IEEE Electron Device Lett.* **21**, 307 (2000).
- ¹²P. A. Wolff, *J. Phys. Chem. Solids* **16**, 184 (1960).
- ¹³S. Yamada and M. Kitao, *Jpn. J. Appl. Phys., Part 1* **32**, 4555 (1993).
- ¹⁴S. Sze, *Physics of Semiconductor Devices* (Wiley, New York, 1981), pp. 45–47.